

clear coactivators in the conventional manner. The allosteric ligand activation and the phosphorylation work synergistically to promote receptor-mediated gene function. Finally, DA reinforces P action through a direct ligand-independent activation of the PR (I) as well as indirectly through activation of DARPP-32. It is implicit that cross-talk between these two pathways is important for integration of the multitude of signals that modulate reproductive behavior.

References and Notes

1. S. K. Mani, J. M. C. Allen, J. H. Clark, J. D. Blaustein, B. W. O'Malley, *Science* **265**, 1246 (1994); E. M. Apostolakis *et al.*, *J. Neurosci.* **16**, 4823 (1996).
2. J. P. Lydon *et al.*, *Genes Dev.* **9**, 2266 (1995).
3. S. K. Mani *et al.*, *Mol. Endocrinol.* **10**, 1728 (1996).
4. P. Greengard *et al.*, *Brain Res. Rev.* **26**, 274 (1998); H. C. Hemmings Jr., P. Greengard, H. Y. L. Tung, P. Cohen, *Nature* **310**, 503 (1984); K. R. Williams, H. C. Hemmings Jr., M. B. LoPresti, W. H. Konigsberg, P. Greengard, *J. Biol. Chem.* **261**, 1890 (1986); P. Greengard, P. B. Allen, A. C. Nairn, *Neuron* **23**, 435 (1999).
5. Ovariectomized female rats were prescreened for sexual receptivity (6) by subcutaneous (sc) administration of EB (2 µg) followed by P (100 µg) 48 hours later. Stereotaxic surgery was performed on sexually receptive rats (6) and mice (3), which were then used in experiments to compare the effects of P, D<sub>1</sub> agonist, and serotonin. Behavioral testing was performed during the dark phase of the reversed light/dark cycle as described (3, 6). The experimental observer was blind to the treatment conditions and mouse genotypes.
6. S. K. Mani *et al.*, *Endocrinology* **135**, 1409 (1994).
7. G. Pollio, P. Xue, A. Zanisi, A. Nicolin, A. Maggi, *Mol. Brain Res.* **19**, 135 (1993); S. Ogawa, U. E. Olazabala, D. W. Pfaff, *J. Neurosci.* **14**, 1766 (1994).
8. A. A. Fienberg *et al.*, *Science* **281**, 838 (1998).
9. EB-induced hypothalamic cytosol PRs in mice carrying the wild-type gene encoding DARPP-32 (+/+) and the null mutation (-/-) were assayed by one-point binding analysis as described previously (3). The following PR concentrations (in fmol/mg of protein) were obtained: vehicle (+/+) = 2.5 ± 1.2; vehicle (-/-) = 2.6 ± 0.87; EB (+/+) = 8.75 ± 1.5; EB (-/-) = 8.4 ± 1.8. Each value is the mean ± SEM of six independent determinations.
10. A. C. Nairn and S. Shenolikar, *Curr. Opin. Neurobiol.* **2**, 296 (1992).
11. P. B. Allen *et al.*, in preparation.
12. Mice homozygous for the I-1 and DARPP-32 targeted mutations were generated by cross-breeding the two mutant lines. Resulting double heterozygotes were then crossed to yield mouse lines homozygous for each mutation and also the corresponding wild-type controls. Additional wild-type and double mutant mice were then generated by inbreeding wild types and double mutants.
13. Rats were decapitated and the brains removed. The hypothalamus was dissected from coronal sections submerged in oxygenated ice-cold artificial cerebrospinal fluid without Ca<sup>2+</sup> or Mg<sup>2+</sup>, and the tissues were processed for cAMP and PKA assays. Sample processing and cAMP assays were performed according to the procedures of Moore *et al.* (20). PKA assays using Kemptide (Leu-Arg-Arg-Ala-Ser-Leu-Gly) as a substrate were carried out with 5 µg of protein as described (27). The amount of cAMP and PKA activity in each sample was normalized to the total amount of protein in the homogenate. Preincubation of protein extracts with the PKA-specific peptide inhibitor Walsh peptide demonstrated a concentration-dependent inhibition of substrate phosphorylation (a substrate:inhibitor ratio of 1:10 = 85% inhibition; 1:100,000 = 15%), confirming that the phosphorylation of the substrate peptide was specific to PKA.
14. P. M. Wise, N. Rance, C. Barraclough, *Endocrinology* **108**, 2186 (1981); I. Vathy and A. M. Etgen, *J. Neu-*

- roendocrinol.* **1**, 383 (1989); J. G. Kohlert, R. K. Rowe, R. L. Meisel, *Horm. Behav.* **32**, 143 (1997).
15. F. Kimura, M. Kawakami, H. Nakano, S. M. McCann, *Endocrinology* **106**, 631 (1980).
16. R. E. Whalen and A. H. Lauber, *Neurosci. Biobehav. Rev.* **10**, 47 (1986); L. Kow, C. V. Mobbs, D. W. Pfaff, *Neurosci. Biobehav. Rev.* **18**, 1 (1994); C. Beyer and G. Gonzalez-Mariscal, *Ann. N.Y. Acad. Sci.* **474**, 270 (1986).
17. Mice were killed by exposure of the head to microwave irradiation for 900 ms, for which a Muromachi Microwave Applicator (Stoelting, Wood Dale, IL) set at 1.5 power was used. The brains were isolated from the crania, and 1-mm coronal sections bracketing the hypothalamic area were prepared with the aid of a mouse brain matrix (Activational Systems, Ann Arbor, MI), following the stereotaxic coordinates of Franklin and Paxinos (22). The microdissection of the hypothalamus was performed as described (23), and the tissues were stored at -80°C until processed. Frozen samples were processed and immunoblotted for phospho-DARPP-32 and total DARPP-32 (24). Phospho-DARPP-32 and total DARPP-32 bands were quantified by densitometry with the use of a PhosphorImager:SF (Molecular Dynamics). The phospho-DARPP-32 values were normalized for the amount of total DARPP-32 present in the samples, and data were represented as percent of vehicle controls. The linear range of signals for densitometry was obtained by exposing the chemiluminescent membranes to x-ray film for varying periods of time. The linearity of measurements was confirmed by calibrating the values obtained to a standard range of phospho-DARPP-32 concentrations in striatal tissues under conditions of basal and D<sub>1</sub> activation. The exposure conditions

that yielded linear measurements for phospho-DARPP-32 were obtained by comparison of phospho-DARPP-32 signals in hypothalamic tissue extracts with those obtained from signals in striatal tissue measurements.

18. J. M. Meredith *et al.*, *J. Neurosci.* **18**, 10189 (1998).
19. R. F. Power, S. K. Mani, J. Codina, O. M. Conneely, B. W. O'Malley, *Science* **254**, 1636 (1991).
20. A. N. Moore, M. N. Waxham, P. K. Dash, *Proc. Natl. Acad. Sci. U.S.A.* **271**, 14214 (1996).
21. E. D. Roberson and J. D. Sweatt, *J. Biol. Chem.* **271**, 30436 (1996).
22. K. B. J. Franklin and G. Paxinos, in *The Mouse Brain in Stereotaxic Coordinates* (Academic Press, San Diego, CA, 1997).
23. J. P. O'Callaghan, K. L. Lavin, Q. Chess, D. H. Clouet, *Brain Res. Bull.* **11**, 31 (1983).
24. G. L. Snyder, G. Fisone, P. Greengard, *J. Neurochem.* **63**, 1766 (1994); A. Nishi, G. L. Snyder, P. Greengard, *J. Neurosci.* **17**, 8147 (1997).
25. Statistical analysis was done by either of the following two methods as appropriate. For each significant analysis of variance (ANOVA), post-hoc comparisons were made using Dunn's method for comparison of all groups versus the control group or the Tukey-Kramer method for multiple comparisons. Instat (Graph Pad, San Diego, CA) was used for statistical analyses.
26. Supported by U.S. Public Health Service grants MH57442 (S.K.M.), MH49662 and NS 35457 (P.K.D.), MH40899 and DA10044 (P.G.), and HD74095 (B.W.O.). We thank P. Ingrassia and J. Ellsworth for excellent assistance.

3 June 1999; accepted 22 December 1999

# Ethanol-Induced Apoptotic Neurodegeneration and Fetal Alcohol Syndrome

Chrysanthy Ikonomidou,<sup>1</sup> Petra Bittigau,<sup>1</sup> Masahiko J. Ishimaru,<sup>2</sup> David F. Wozniak,<sup>3</sup> Christian Koch,<sup>1</sup> Kerstin Genz,<sup>1</sup> Madelon T. Price,<sup>3</sup> Vanya Stefovskaja,<sup>1</sup> Friederike Hörster,<sup>1</sup> Tanya Tenkova,<sup>3</sup> Krikor Dikranian,<sup>3</sup> John W. Olney<sup>3\*</sup>

The deleterious effects of ethanol on the developing human brain are poorly understood. Here it is reported that ethanol, acting by a dual mechanism [blockade of N-methyl-D-aspartate (NMDA) glutamate receptors and excessive activation of GABA<sub>A</sub> receptors], triggers widespread apoptotic neurodegeneration in the developing rat forebrain. Vulnerability coincides with the period of synaptogenesis, which in humans extends from the sixth month of gestation to several years after birth. During this period, transient ethanol exposure can delete millions of neurons from the developing brain. This can explain the reduced brain mass and neurobehavioral disturbances associated with human fetal alcohol syndrome.

Intrauterine exposure of the human fetus to ethanol causes a neurotoxic syndrome (I) termed fetal alcohol effects (FAE) or fetal alcohol syndrome (FAS), depending on severity.

The most disabling features of FAE/FAS are neurobehavioral disturbances ranging from hyperactivity and learning disabilities to depression and psychosis (2, 3). It is thought that the brain is particularly sensitive to the neurotoxic effects of ethanol during the period of synaptogenesis, also known as the brain growth spurt period, which occurs postnatally in rats but prenatally (during the last trimester of gestation) in humans (4-6). Thus, ethanol treatment of neonatal rats causes reproducible effects relevant to FAE/FAS, including a generalized loss

<sup>1</sup>Department of Pediatric Neurology, Charité, Virchow Clinics, Humboldt University, Augustenburger Platz 1, 13353 Berlin, Germany. <sup>2</sup>Medical Research Institute, Tokyo Medical and Dental University, 2-3-10 Kanda-surugadai, Chiyodoku, Tokyo, Japan. <sup>3</sup>Department of Psychiatry, Washington University School of Medicine, 4940 Children's Place, St. Louis, MO 63110, USA.

\*To whom correspondence should be addressed.

## REPORTS

of brain mass and a specific loss of cerebellar and hippocampal neurons (7, 8). However, these circumscribed losses cannot account for the overall loss of brain mass, and the mechanism(s) underlying ethanol's injurious effects on the developing brain remain a mystery.

Having recently found (9) that transient blockade of NMDA glutamate receptors during the period of synaptogenesis causes widespread apoptotic neurodegeneration in the infant rat brain, we decided to evaluate ethanol, a known NMDA antagonist (10), for its ability to trigger apoptotic neurodegeneration in the developing rat brain. A 20% solution of ethanol in normal saline was administered to 7-day-old Sprague-Dawley rats in two separate treatments, 2 hours apart, each treatment delivering 2.5 g/kg subcutaneously (sc); control rats were treated with saline only. The brains were examined histologically 24 hours after the first treatment. In the brains of saline-treated rats, both silver staining and TUNEL (terminal deoxynucleotidyl transferase-mediated deoxyuridine triphosphate nick-end labeling) (11–13) revealed a very light pattern of neurodegeneration attributable to physiological cell death (PCD), the apoptotic process by which biologically redundant neurons are deleted from the developing brain. In the brains of ethanol-treated rats, these stains revealed a very dense and widely distributed pattern of neurodegeneration, a pattern that overlapped with but was more extensive than that (9) induced by other NMDA antagonists (Fig. 1, A to H). As assessed by electron microscopy, the ethanol-induced cell death process clearly met ultrastructural criteria (14, 15) for apoptosis (Fig. 1L).

Quantitative evaluation (16, 17) revealed that the densities of degenerating neurons in saline-treated rats varied from 0.13 to 1.55% of the total neuronal density in brain regions examined (Table 1). This represents the rate of spontaneous apoptosis (PCD) that occurs naturally in the rat brain at postnatal day 8 (P8). In

contrast, the densities of degenerating neurons in ethanol-treated pups ranged from 5 to 30% of the total neuronal densities in the same brain regions. The mean number ( $\pm$ SEM) of degenerating neurons in selected regions of the forebrain (16) was 12,567,726  $\pm$  1,008,195 for the ethanol-treated rats ( $n = 6$ ), compared to

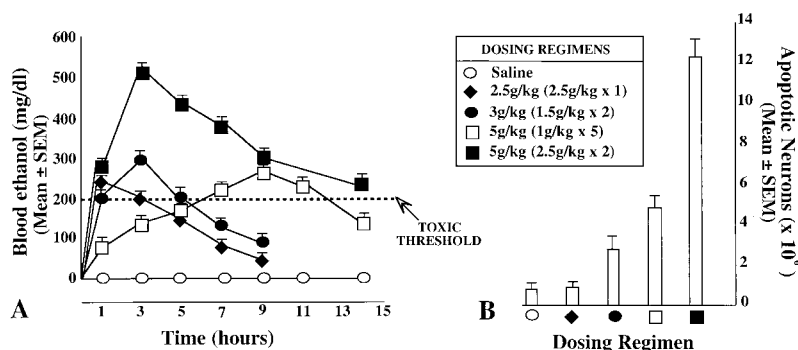


**Fig. 2.** Ethanol was administered to P7 rats by several dosing regimens. The total dose ranged from 0 to 5 g/kg sc and was administered either in a single injection or in multiple injections spaced 2 hours apart. (A) Blood ethanol curves associated with each of several dosing regimens. (B) Severity of apoptotic neurodegeneration associated with each dose–blood ethanol curve. The histographic values in (B) represent total numbers of apoptotic neurons (means  $\pm$  SEM,  $n = 6$  per group) in the forebrains of saline- and ethanol-treated rats. Severity of degeneration was established using silver-stained sections and by counting argyrophilic profiles in 13 brain regions, as described (16). Many blood ethanol curves not shown were generated; those shown were selected because each is representative of a type of curve required to trigger a certain amount of apoptotic neurodegeneration. The data show that the severity of apoptotic degeneration does not correlate with total dose, but rather with the rate at which the dose is given and the length of time the blood ethanol level remains elevated above a toxic threshold in the range of 200 mg/dl. Dosing regimens that produced blood ethanol concentrations that did not exceed 200 mg/dl for more than 2 hours did not increase the rate of apoptotic neurodegeneration significantly above the spontaneous rate in saline-treated rats. If blood ethanol concentrations exceeded 200 mg/dl for 4 hours, apoptotic neurodegeneration was significantly increased, and if concentrations exceeded 200 mg/dl for more than 4 hours, the degenerative response became progressively more severe in proportion to the length of time the concentrations exceeded 200 mg/dl.

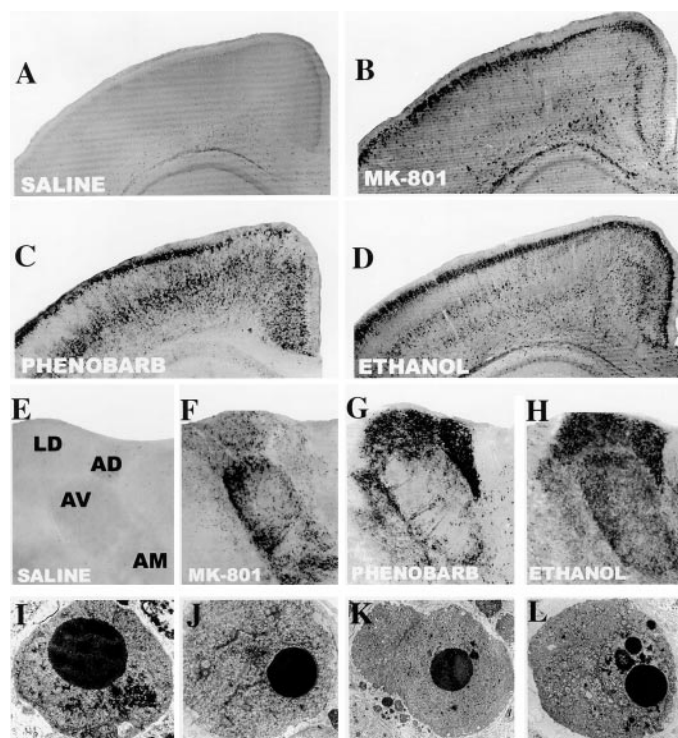
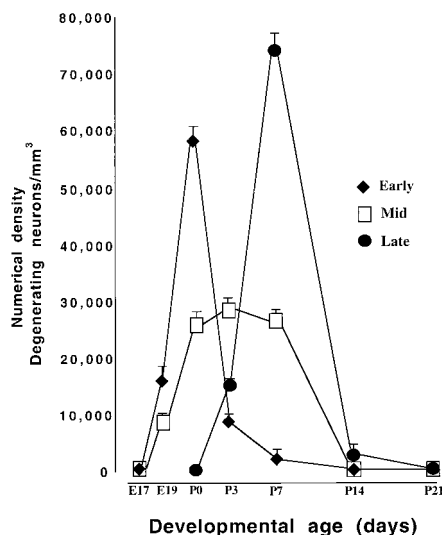


**Fig. 1.** (A to D) Low-magnification (25 $\times$ ) light microscopic overviews of silver-stained (11–13) transverse sections from the parietal and cingulate cortex of P8 rats treated 24 hours previously with saline, MK-801 (NMDA antagonist), phenobarbital, or ethanol. Degenerating neurons (small dark dots) are abundantly present in several brain regions after treatment with MK-801, phenobarbital, or ethanol, but are only sparsely present after saline treatment. Note that MK-801 and phenobarbital both affect neurons superficial to the cortical surface, whereas the middle cortical layers are affected very prominently by phenobarbital and are relatively spared by MK-801. The ethanol pattern resembles a combination of the MK-801 and phenobarbital patterns. (E to H) Light micrographs (55 $\times$ ) depicting the anterior thalamus at the level of the laterodorsal (LD), anterodorsal (AD), anteroventral (AV), and anteromedial (AM) nuclei, respectively. Note that MK-801 affects the LD, AV, and AM nuclei but not the AD nucleus, whereas phenobarbital affects the LD and AD nuclei very prominently but almost entirely spares the AV and AM nuclei. The ethanol pattern includes all four nuclei, as would be expected if it acts by a dual mechanism involving blockade of NMDA receptors plus activation of GABA<sub>A</sub> receptors. (I to L) Electron micrographs (1800 $\times$ ) illustrating that apoptotic neurodegeneration induced by MK801 (J), phenobarbital (K), or ethanol (L) has the same ultrastructural appearance as PCD (I), an apoptotic phenomenon that occurs spontaneously in the developing brain. As we have recently described (9, 14), in both spontaneous and induced apoptosis, the earliest signs are the formation of spherical chromatin masses and flocculent densities in the nucleus while the nuclear envelope remains intact and cytoplasmic organelles are relatively unaltered; this is followed in the middle and late stages by fragmentation of the nuclear envelope, intermixing of nucleoplasmic and cytoplasmic contents, and progressive condensation of the entire cell. All four examples shown here have a similar appearance, as they are all in the middle stage of apoptotic neurodegeneration.

## REPORTS

**Fig. 3.** Age dependency of ethanol-induced apoptosis in the brains of developing rats. Immature rats were exposed at different developmental ages (E17 to P21) to saline or ethanol (2.5 g/kg sc at 0 and 2 hours; total dose 5 g/kg), and 24 hours later we used the stereological disector method (16, 17) to assess the numerical densities of degenerating neurons in DeOlmos silver-stained sections of various brain regions. To determine the apoptotic degeneration that could be attributed to ethanol, we subtracted the mean numerical density count for the saline-treated rats ( $n = 6$ ) in a given brain region from the mean numerical density count for the ethanol-treated rats ( $n = 6$ ) in the same brain region. In each brain region there was a time window during which neurons showed vulnerability to ethanol-induced apoptosis, and the timing of this vulnerability period was different for different brain regions. However, each region displayed a temporal profile that fit into an early-, middle-, or late-stage category. Neuronal populations showing the early-stage profile (ventromedial hypothalamus, mediodorsal and ventral thalamus) began to display a significant response to ethanol on day E19, which reached a peak at P0 and rapidly declined thereafter. Neurons showing the middle-stage profile (subiculum, hippocampus, caudate, and laterodorsal and anteroventral thalamus) began to show a response on E19, which reached a peak at P3 and gradually declined to zero by P14. Those showing the late-stage profile (frontal, parietal, temporal, cingulate, and retrosplenial cortices) exhibited a degenerative response that began on day P3, peaked at P7, was markedly diminished at P14, and was absent at P21. Each of the curves presented here pertains to a single brain region that is representative of a response pattern: ventromedial hypothalamus, early stage; laterodorsal thalamus, middle stage; and frontal cortex, layer II, late stage.



835,360 ± 101,079 for the saline-treated group ( $n = 6$ ).

In additional experiments with P7 rats, we administered ethanol by various dosing regimens and compared the severity of the apoptotic response (16) with the blood ethanol curves produced by each regimen. We found that the apoptotic response induced by ethanol cannot be predicted by the dose, but rather depends on how rapidly the dose is administered and on how long the blood ethanol levels are elevated above a toxic threshold in the range of 180 to 200 mg/dl (Fig. 2). Maintaining blood ethanol concentrations at or above 200 mg/dl for four consecutive hours was the minimum condition for triggering neurodegeneration. If ethanol concentrations remained above 200 mg/dl for more than 4 hours, the degenerative response became progressively more severe and more widespread in proportion to the length of time that the concentrations remained above this level.

To determine how the apoptotic response to ethanol might differ as a function of developmental age, we administered either saline or ethanol (2.5 g/kg sc at 0 and 2 hours; total dose 5 g/kg) to pregnant rats on embryonic day 17 (E17) or E19 or to their offspring on P0, P3, P14, or P21; after 24 hours, we

**Table 1.** Rate of apoptotic neurodegeneration in 15 brain regions of P8 rats 24 hours after treatment with saline, ethanol, diazepam, or MK801.

Brain region	Saline		Ethanol*: Degenerating cell density as percentage of total cell density (mean ± SEM)	Diazepam*: Degenerating cell density as percentage of total cell density (mean ± SEM)	MK801*: Degenerating cell density as percentage of total cell density (mean ± SEM)
	Numerical density, total cells (mean/mm³ ± SEM)	Degenerating cell density as percentage of total cell density (mean ± SEM)			
CA1 hippocampus	220,050 ± 4,584	0.85 ± 0.11	17.35 ± 1.36	8.00 ± 1.31	3.35 ± 0.67
Subiculum	198,124 ± 8,205	0.59 ± 0.04	16.48 ± 1.60	13.47 ± 2.75	10.70 ± 1.72
Caudate	242,534 ± 11,140	0.29 ± 0.04	8.07 ± 0.50	3.97 ± 0.92	4.77 ± 0.85
Laterodorsal thalamus	133,945 ± 13,148	0.30 ± 0.05	18.33 ± 2.72	11.79 ± 1.99	11.91 ± 2.21
Mediodorsal thalamus	199,335 ± 6,398	0.40 ± 0.01	5.02 ± 1.17	5.51 ± 1.34	2.39 ± 0.34
Septum	107,143 ± 9,510	0.31 ± 0.05	10.31 ± 0.79	5.82 ± 0.38	3.30 ± 0.81
Pallidum	214,286 ± 21,087	0.13 ± 0.03	5.43 ± 0.81	3.50 ± 0.19	2.09 ± 0.19
Frontal cortex layer II	219,432 ± 4,541	1.55 ± 0.18	24.62 ± 2.28	7.47 ± 0.96	22.65 ± 1.93
Frontal cortex layer IV	142,120 ± 10,323	0.20 ± 0.05	4.91 ± 0.34	3.89 ± 0.95	1.43 ± 0.18
Parietal cortex layer II	223,900 ± 13,434	1.08 ± 0.28	25.38 ± 2.03	10.69 ± 2.42	26.13 ± 2.51
Parietal cortex layer IV	156,078 ± 6,323	0.22 ± 0.05	5.70 ± 0.55	3.84 ± 0.73	1.72 ± 0.26
Cingulate cortex layer II	218,932 ± 11,239	1.54 ± 0.21	26.73 ± 2.72	9.36 ± 0.27	15.49 ± 1.79
Cingulate cortex layer IV	148,100 ± 6,125	0.13 ± 0.03	13.72 ± 0.87	11.81 ± 1.54	3.22 ± 0.85
Retrosplenial cortex layer II	235,948 ± 13,857	0.89 ± 0.07	29.87 ± 1.60	13.38 ± 1.17	11.49 ± 1.82
Retrosplenial cortex layer IV	143,250 ± 10,857	0.33 ± 0.08	11.70 ± 0.98	5.47 ± 1.29	5.95 ± 0.42

\*In all brain regions, the rate of apoptosis was significantly higher ( $P < 0.001$ ) in rats treated with ethanol (2.5 g/kg × 2) ( $n = 7$ ), diazepam (30 mg/kg × 1) ( $n = 6$ ), or MK801 (0.5 mg/kg × 3) ( $n = 6$ ) than in rats treated with saline ( $n = 5$ ). For all comparisons (ethanol, diazepam, or MK801 versus saline), the  $P$  values exceeded the Bonferroni corrected levels ( $P = 0.05/45 = 0.0011$ ).

compared the neurodegenerative response in the fetal or infant brains with the response in P7 rats. To assess the degenerative response to ethanol, we compared the density of degenerating neurons in various brain regions of saline-treated rats with the density of degenerating neurons in the same brain regions of ethanol-treated rats. We found that there is a time window from E19 to P14 when various neurons in the forebrain show transient sensitivity to ethanol-induced neurodegeneration, and within this period, which coincides with the synaptogenesis period, different neuronal populations display transient sensitivity at different times. Three response patterns were observed (Fig. 3).

To assess whether the apoptotic response to ethanol is associated with a loss of brain mass, we administered saline or ethanol (2.5 g/kg sc at 0 and 2 hours; total dose 5 g/kg) to infant rats on P7 and found, when the experiment was terminated at P12, that the brain weights (whole brain or forebrain and cerebellum weighed separately) of the ethanol-treated rats were significantly lower than those of the saline-treated rats (Fig. 4).

Because ethanol triggered apoptosis in some brain regions that are not typically affected by NMDA antagonists, we attempted to identify other possible mechanisms to explain ethanol's effects in these brain regions. In a series of experiments (18), we were unable to demonstrate an appreciable apoptotic response to agents that act as either agonists or antagonists at dopamine receptors, block kainic acid or muscarinic cholinergic receptors, or block voltage-gated ion channels. However, a robust apoptotic response

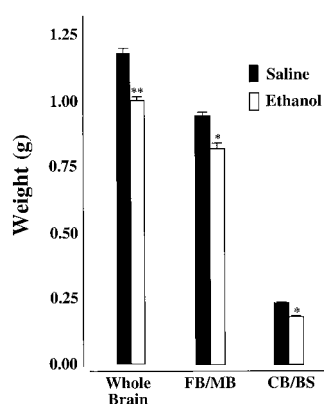


**Fig. 4.** On day P12, the brains of rats that were treated with saline ( $n = 6$ ) or ethanol ( $n = 6$ ) on day P7 were weighed to obtain a whole brain weight, then were dissected at the level of the pons into two portions, one including the forebrain (FB) and midbrain (MB) and the other including the cerebellum (CB) and brainstem (BS). Sampling and weighing of the brains were performed in a blinded manner. The weights for the ethanol-treated brains (whole or in parts) were significantly lower than those for the saline-treated brains (\* $P < 0.05$ , \*\* $P < 0.01$ ; Student's  $t$  test).

was triggered by benzodiazepines and barbiturates, "GABAergic" agents that either mimic or potentiate the action of GABA at GABA<sub>A</sub> receptors. The agents tested were diazepam [10 to 30 mg/kg intraperitoneally (ip) at 0 hours,  $n = 6$ ], clonazepam (0.5 to 4 mg/kg ip at 0 hours,  $n = 6$ ), pentobarbital (10 mg/kg ip at 0 and 4 hours,  $n = 6$ ), and phenobarbital (50 to 75 mg/kg ip at 0 hours,  $n = 6$ ). These agents, in a dose-dependent manner, triggered widespread cell death in the infant rat brain, which was apoptotic as assessed by ultrastructural analysis (Fig. 1K). The pattern of degeneration was similar for each GABAergic agent, but this pattern differed in several major respects from that induced by NMDA antagonists (Fig. 1, A to H). However, superimposing one pattern on the other resulted in a composite pattern closely resembling that induced by ethanol. We also studied the window of vulnerability to the proapoptotic actions of diazepam and phenobarbital, and we determined that it coincides with the period of synaptogenesis.

Our results show that exposure of the developing rat brain to ethanol for a period of hours during a specific developmental stage (synaptogenesis) predictably induces an apoptotic neurodegenerative reaction that deletes large numbers of neurons from several major regions of the developing brain. Of ethanol's many actions in the brain, it appears that two—its blocking action at NMDA glutamate receptors and its positive modulatory action at GABA<sub>A</sub> receptors—are primarily responsible for its proapoptotic effects. In addition, the developmental period during which the immature brain is vulnerable to the proapoptotic action of NMDA antagonists, GABAergic agents, and ethanol is the same: For all three, it coincides with the synaptogenesis period.

In humans, as noted earlier, the period of synaptogenesis occurs prenatally, during the last 3 months of gestation (6). If a pregnant mother imbibes ethanolic beverages for several hours in a single drinking episode, she could expose her third-trimester fetus to blood ethanol levels equivalent to those required to trigger apoptotic neurodegeneration in the immature rat brain (200 mg/dl lasting 4 hours or more).

From a clinical perspective, it is important to recognize that both NMDA antagonists and GABA<sub>A</sub> agonists are frequently used as sedatives, tranquilizers, anticonvulsants, or anesthetics in pediatric and/or obstetric medicine. These agents also are drugs of abuse. Because the human brain growth spurt spans not only the last trimester of pregnancy but several years after birth (6), the developing human brain may be exposed to these agents by medical professionals or by drug-abusing pregnant mothers. Also relevant is our observation that within the synaptogenesis period, different neuronal pop-

ulations have different temporal patterns of response to the apoptosis-inducing effects of these drugs. Thus, depending on the timing of exposure, different combinations of neuronal groups will be deleted, which signifies that this is a neurodevelopmental mechanism that can contribute to a wide spectrum of neuropsychiatric disturbances.

**References and Notes**

1. K. L. Jones and D. W. Smith, *Lancet* **ii**, 999 (1973); \_\_\_\_\_, C. N. Ulleland, A. P. Streissguth, *Lancet* **i**, 1267 (1973); S. K. Clarren, A. C. Alvord, S. M. Sumi, A. P. Streissguth, D. W. Smith, *J. Pediatr.* **92**, 64 (1978); V. W. Swayze et al., *Pediatrics* **99**, 232 (1977).
2. S. K. Clarren and D. W. Smith, *N. Engl. J. Med.* **298**, 1063 (1978); K. A. Kerns, A. Don, C. A. Mateer, A. P. Streissguth, *J. Learn. Disab.* **30**, 685 (1977); K. K. Sulik, M. C. Johnston, M. A. Webb, *Science* **214**, 936 (1981); C. Famy, A. P. Streissguth, A. S. Unis, *Am. J. Psychiatr.* **155**, 552 (1998).
3. M. J. Eckardt et al., *Alcohol. Clin. Exp. Res.* **22**, 998 (1998); C. L. Faingold, P. N'Gouemo, A. Riaz, *Prog. Neurobiol.* **55**, 509 (1998); D. W. Sapp and H. H. Yeh, *J. Pharmacol. Exp. Ther.* **284**, 768 (1998).
4. C. R. Goodlett and J. R. West, in *Maternal Substance Abuse and the Developing Nervous System*, I. Zagon and T. Slotkin, Eds. (Academic Press, San Diego, CA, 1992), pp. 45–75.
5. J. R. West, *Alcohol Drug Res.* **7**, 423 (1987).
6. J. Dobbing and J. Sands, *Early Hum. Dev.* **3**, 79 (1979).
7. J. R. West, K. M. Hamre, M. D. Cassell, *Alcohol. Clin. Exp. Res.* **10**, 190 (1986).
8. C. Bauer-Moffett and J. Altman, *Brain Res.* **119**, 249 (1977); C. R. Goodlett, B. L. Marcussen, J. R. West, *Alcohol* **7**, 107 (1990); A. E. Ryabinin, M. Cole, F. E. Bloom, M. C. Wilson, *Alcohol. Clin. Exp. Res.* **19**, 784 (1995).
9. C. Ikonomidou et al., *Science* **283**, 70 (1999).
10. D. M. Lovinger, G. White, F. F. Weight, *Science* **243**, 1721 (1989); P. L. Hoffman, C. S. Rabe, F. Moses, B. Tabakoff, *J. Neurochem.* **52**, 1937 (1989).
11. Twenty-four hours after saline or ethanol treatment, the immature rats were deeply anesthetized and perfused with aldehyde fixative, and the brains were studied with the use of three histological methods: TUNEL, DeOlmos silver impregnation, and electron microscopy. The TUNEL method, first described by Gavrieli et al. (12), detects a DNA fragmentation process that occurs typically in cells that are dying by an apoptotic mechanism. Thus, it is useful for marking neurons that are undergoing experimentally induced apoptosis or neurons in the normal brain that are undergoing PCD. We have found (9, 14) that DeOlmos silver impregnation (13) also stains neurons undergoing either experimentally induced apoptosis or PCD, and that it reveals in the normal brain the same pattern of cells dying by PCD that is revealed by TUNEL. The DeOlmos silver method is more favorable for quantitative purposes because it more uniformly penetrates thick histological sections. Because neither TUNEL nor the DeOlmos method is specific for apoptosis (they are positive for apoptosis but also for at least some nonapoptotic cell death processes), it is necessary to establish the apoptosis diagnosis by ultrastructural analysis, using as a reference standard the ultrastructural appearance of neurons undergoing PCD in the normal developing rat brain (14).
12. Y. Gavrieli, Y. Sherman, S. A. Ben-Sasson, *J. Cell Biol.* **119**, 493 (1992).
13. J. S. DeOlmos and W. R. Ingram, *Brain Res.* **33**, 523 (1971).
14. M. J. Ishimaru et al., *J. Comp. Neurol.* **408**, 461 (1999).
15. A. H. Wyllie, J. F. R. Kerr, A. R. Currie, *Int. Rev. Cytol.* **68**, 251 (1980).
16. In the normal developing brain, after neurons have differentiated, migrated, and are undergoing synaptogenesis, spontaneous apoptotic neurodegeneration (PCD) occurs at a relatively low rate, about 1% of the total neuronal population (9). To determine whether ethanol treatment induced a rate of apoptotic neu-

rodgeneration exceeding the spontaneous rate in a given brain region, we used an unbiased stereological disector method (17) to quantify the numerical density (neurons/mm<sup>3</sup>) of normal neurons in 70- $\mu$ m Nissl-stained sections, or of degenerating neurons in 70- $\mu$ m sections stained by the DeOlmos silver method (13). A total of 8 to 10 disectors (0.05 mm by 0.05 mm, disector height 0.07 mm) were used to sample each brain region. Counts were performed in a blinded manner. To establish the absolute numbers of degenerating neurons, we identified boundaries of individual brain regions [thalamus, dentate gyrus, CA1 hippocampus, subiculum, caudate, septum, hypothalamus, amygdala, and frontoparietal, cingulate, retrosplenial, temporal, and pyriform/entorhinal cortices, according to G. Paxinos, I. Tork, L. H. Tecott, K. L. Valentino, *Atlas of the Developing Rat Brain* (Academic Press, New York, 1991)] in Nissl-stained sections. We used an image analysis system (IMAGE 1.54, National Institutes of Health) to facilitate volume determinations for each brain region. Multiplication of the volume of a given region by the numerical density of degenerating neurons in that region

provided an estimate of total numbers of neurons deleted from each brain region by ethanol treatment. The regional values were summed to give a total for each brain, and from these totals, means ( $\pm$ SEM) were calculated separately for the brains in the ethanol- and saline-treated groups.

17. M. J. West, *Neurobiol. Aging* **14**, 275 (1993); H. J. G. Gundersen, T. F. Bendtsen, L. Korbo, M. J. West, *APMIS* **96**, 379 (1988).
18. In addition to GABAergic agents, we tested 6-nitro-7-sulfamoylbenzo[f]quinoxaline-2,3-dione (NBQX), an antagonist of non-NMDA glutamate receptors, at a dose of 20 mg/kg ip given at 0, 75, and 150 min and at 8 hours ( $n = 5$ ); scopolamine hydrobromide, an antagonist of cholinergic muscarinic receptors, at a dose of 0.3 mg/kg ip given at 0, 4, and 8 hours ( $n = 5$ ); haloperidol, an antagonist of dopamine receptors, at a dose of 10 mg/kg ip given at 0 and 8 hours ( $n = 5$ ); and L-dopa, an agent that increases the availability of dopamine at dopamine receptors, administered at 50, 100, or 200 mg/kg ip together with benserazide (dopamine decarboxylase inhibitor) at 14, 28, or 56 mg/kg ip ( $n = 5$  per dose). Finally, because NMDA

receptor-activated ion channels are highly permeable to Ca<sup>2+</sup> ions, we tested whether blockade of calcium influx via other routes (i.e., voltage-dependent Ca<sup>2+</sup> channels) may also cause apoptotic neurodegeneration in the brain. For this purpose we treated P7 rats with the Ca<sup>2+</sup> channel blockers nimodipine (50 mg/kg ip at 0 and 8 hours;  $n = 6$ ) or nifedipine (10 mg/kg ip at 0 and 8 hours;  $n = 6$ ). We examined the brains histologically 24 hours after each of these treatments. None of these agents reproduced the apoptosis-inducing action of NMDA antagonists.

19. Supported in part by Deutsche Forschungsgemeinschaft grant Ik2/2-1, Humboldt University grant 98-649, National Institute for Mental Health Research Scientist Award MH 38894 (J.W.O.), National Institute on Aging grant AG 11355, National Institute on Drug Abuse grant DA 05072, National Eye Institute grant EY 08089, and a National Alliance for Research on Schizophrenia and Depression Established Investigator Award (J.W.O.).

3 August 1999; accepted 21 December 1999

## Evidence for DNA Loss as a Determinant of Genome Size

Dmitri A. Petrov,<sup>1\*</sup> Todd A. Sangster,<sup>2</sup> J. Spencer Johnston,<sup>3</sup> Daniel L. Hartl,<sup>2</sup> Kerry L. Shaw<sup>2</sup>

Eukaryotic genome sizes range over five orders of magnitude. This variation cannot be explained by differences in organismic complexity (the C value paradox). To test the hypothesis that some variation in genome size can be attributed to differences in the patterns of insertion and deletion (indel) mutations among organisms, this study examines the indel spectrum in *Laupala* crickets, which have a genome size 11 times larger than that of *Drosophila*. Consistent with the hypothesis, DNA loss is more than 40 times slower in *Laupala* than in *Drosophila*.

Wide variation in eukaryotic genome size is a pervasive feature of genome evolution. Large differences in haploid DNA content (C value) are found within protozoa (5800-fold range), arthropods (250-fold), fish (350-fold), algae (5000-fold), and angiosperms (1000-fold) (1). This variation is called the C value paradox (2, 3) because genome size is not correlated with the structural complexity of organisms or with the estimated number of genes. Despite much progress in the study of genomes, the C value paradox remains largely unresolved.

*Drosophila* species, which have small genomes, spontaneously lose DNA at a much higher rate than mammalian species, which have large genomes (4–7). Although many mechanisms can affect genome size—including polyploidy, fixation of accessory chromosomes or large duplications (8), and expan-

sions of satellite DNA or transposable elements (9)—the *Drosophila* findings suggest that some differences in haploid genome size may result from variation in the rate of spontaneous loss of nonessential DNA (4). Here, we test this hypothesis by examining the indel spectrum in Hawaiian crickets (*Laupala*), which have a genome size ~11-fold larger than that of *Drosophila* (10). Specifically, we test the prediction of a lower rate of DNA loss in *Laupala* than in *Drosophila*, corresponding to the large difference in genome size.

Sequences unconstrained by natural selection exhibit patterns of substitution, reflecting the underlying spectra of spontaneous mutations (11). As pseudogene surrogates we chose nontransposing copies of non-LTR (long terminal repeat) retrotransposable elements (4, 12). Transposition of non-LTR elements usually results in a 5'-truncated copy that is unable to transpose because of lack of a promoter and lack of the capacity to encode functional proteins (13, 14); these “dead-on-arrival” (DOA) elements are essentially pseudogenes.

We identified a new non-LTR element in *Laupala*, here designated *Lau1*, by means of polymerase chain reaction (PCR) with degen-

erate primers to conserved regions of the non-LTR reverse transcriptase (15). Evolution of unconstrained DOA elements can be distinguished from that of the constrained, active elements via phylogenetic analysis of nucleotide sequences of individual DOA elements (4, 12). Substitutions in a transpositionally active lineage are represented in multiple DOA elements generated by transposition of the active copy, whereas substitutions in each DOA lineage are unique (barring parallel mutations) because of the inability of DOA elements to transpose. This implies that, in a gene tree of non-LTR sequences from closely related species, the active lineages map to internal branches (identified through substitutions shared among elements), whereas DOA lineages map to terminal branches (identified through unique substitutions). Some DOA lineages may also map to internal branches, because elements from different species may be identical by descent (IBD) because of transmission of the same (allelic) DOA copy from a common ancestor (7, 12). Nevertheless, as long as the number of active lineages is small and the sampling is dense, substitutions in the terminal branches will correspond primarily to the DOA element evolution (12).

If the terminal branches of the *Lau1* gene tree (Fig. 1) represent unconstrained evolution of DOA elements, we predict the absence of purifying selection operating along these branches. Confirming this prediction, point substitutions in terminal branches map with equal frequencies to all three codon positions (*G* test;  $P = 0.64$ ). In addition, the terminal branches feature numerous element-specific indels (48 deletions and 18 insertions in 49 terminal branches). The internal branches show evidence of relaxed selection as well, which suggests that many elements in our sample are IBD through inheritance of ancestral allelic DOA copies. The substitutions in the internal branches are found at equal fre-

<sup>1</sup>Harvard University Society of Fellows, <sup>2</sup>Department of Organismic and Evolutionary Biology, Harvard University, Cambridge, MA 02138, USA. <sup>3</sup>Department of Entomology, Texas A&M University, College Station, TX 77843, USA.

\*To whom correspondence should be addressed. E-mail: dpetrov@oeb.harvard.edu